RSC Advances

ROYAL SOCIETY OF CHEMISTRY

www.rsc.org/advances

Growth Kinetics and Wettability Conversion of Vertically-aligned ZnO Nanowires Synthesized by Hydrothermal Method

S. L. Cheng [a,b] *, J. H. Syu [a], S. Y. Liao [a], C. F. Lin [a], and P. Y. Yeh [a]

[a] Department of Chemical and Materials Engineering, National Central University, Chung-Li District, Taoyuan City, Taiwan, R.O.C.

[b] Institute of Materials Science and Engineering, National Central University, Chung-Li District, Taoyuan City, Taiwan, R.O.C.

Abstract

We report here the first study of growth kinetics of vertically-aligned ZnO nanowire arrays grown on Al-doped ZnO (AZO) seed layer-coated substrates by hydrothermal method. The as-synthesized vertical ZnO nanowires possess a single-crystalline wurtzite structure and a preferred growth orientation along the [0001] direction. The ZnO nanowires were found to grow following the reaction-controlled process and their lengths can be tuned from several to over ten micrometers by adjusting the hydrothermal temperatures and time. By measuring the growth rates at different synthesis temperatures, the activation energy for the linear growth of vertical ZnO nanowires on AZO-seeded substrates derived from the slope of the Arrhenius plot was around 35 kJ/mol. The obtained value is smaller than that of ZnO nanowires grown in bulk solution, which can be explained by the different nucleation mechanisms. From water contact angle measurements, it is found that the as-synthesized ZnO nanowires are hydrophilic in nature, and their surface wettability

can be adjusted by the storage time and heat treatment conditions. Furthermore, the reversible switching of the surface wettability of ZnO nanowires has been accomplished by alternate annealing in vacuum and oxygen atmospheres. The ZnO nanowires with switchable surface wettability will find promising applications in surface engineering.

* Corresponding author.
Tel: *+886-3-4227151 ext.34233* ; Fax: *+886-3-2804510*.
E-mail: *slcheng@ncu.edu.tw* (S. L. Cheng).

1. Introduction

Recently, nanostructured metal oxide materials, particularly one-dimensional nanostructures have attracted a lot of attention due to their variety of potential applications and distinct physical and chemical properties compared with their bulk counterparts.[1,2] Of the various metal oxide semiconductor nanomaterials, one-dimensional zinc oxide (ZnO) based nanostructures has been extensively studied as a n-type semiconductor with a wide direct band gap and broadly applied in optoelectronic devices, photovoltaic cells, nanogenerators, and gas sensors.[3-5] To synthesize large-scale ZnO-based nanowires on desired substrates, various physical (e.g. thermal evaporation, pulsed laser deposition),[6,7] chemical (e.g. MOCVD, solvothermal process),[8,9] and electrochemical (e.g. electrodeposition)[10,11] synthetic techniques have been developed. Among these approaches, the hydrothermal route is probably one of the most convenient and cost-effective methods for the synthesis of ZnO-based nanowires.[12-14] Contrasted with the above-mentioned methods, the whole hydrothermal synthesis process is carried out in aqueous solution without the need of using ignitable precursors, additional power sources, expensive and complicated apparatuses, and high vacuum or high operation temperature conditions. Thus, the hydrothermal method is particularly suitable for both rigid inorganic and flexible organic substrates due to its low reaction temperatures.

Several studies have demonstrated that with the wet-chemical hydrothermal approaches, large-scale ZnO nanowires were successfully synthesized in low temperature ranges of 55 - 150 ℃.[15-18] It is worth mentioning that although numerous works have been conducted to synthesize ZnO nanowires by using the hydrothermal method, the corresponding studies related to the growth

kinetics of ZnO nanowires synthesized under different hydrothermal conditions are rather scarce. To our knowledge, the study reported by Zhou et al.[18] is the only one that systematically investigated the kinetics of ZnO nanorod growth in a bulk solution. However, it should be noted from their study that all the synthesized ZnO nanorods were singly dispersed in the hydrothermal solution at random positions. Up to now, the study on the growth kinetics of vertically-aligned ZnO nanowire arrays grown on solid substrates has not yet been performed and reported. Surface wettability is a fundamental characteristic of solid state materials that plays important roles in many practical applications, such as self-cleaning, corrosion resistance, drug delivery, and anti-fogging.[19-21] The ability to control a solid surface having specific wettability is therefore absolutely essential. The surface wettability of ZnO-based materials has been studied extensively, and several reports have shown that the ZnO surfaces would become more hydrophilic with increasing the density of surface oxygen vacancies.[22,23] Since the growth kinetic data are necessary to provide crucial information for understanding and controlling the formation process of ZnO nanowires on solid substrates, and the surface wettability of nanowires are known to be significantly affected by their surface compositions and morphologies, it is of great importance to investigate the growth kinetics of vertically-aligned ZnO nanowires under different experimental conditions and the corresponding surface wetting behaviors.

In this paper, we report the successful synthesis of length-tunable ZnO nanowires with controllable wettability on Al-doped ZnO seeded (AZO-seeded) substrates by using a hydrothermal method and heat treatments. Systematic investigations on the growth kinetic, surface

morphology, microstructure, crystallographic orientation, and the mechanism of wettability conversion of vertical ZnO nanowire arrays produced under different experimental conditions have been carried out.

2. Experimental

Square pieces 10 × 10 mm^2 in size were cut from glass plates (Corning Eagle2000) or (001)Si wafers to be used as the deposition substrates in this study. All of these substrates were ultrasonic cleaning in acetone, isopropyl alcohol, and deionized (DI) water, respectively, for 20 min and then blow-dried with nitrogen gas. A 200-nm-thick AZO film was deposited onto the substrates by radio-frequency (RF) magnetron sputtering at room temperature to act as the seed layer during the subsequent hydrothermal synthesis process. The base pressure in the sputtering chamber was better than 1×10^{-5} torr. The as-deposited AZO seed layer was then annealed in vacuum ($< 2 \times 10^{-2}$ torr) at 400 ℃ for 1 h to improve its crystallinity. The hydrothermal synthesis of vertically-aligned ZnO nanowires was carried out by immersing the AZO-seeded substrates into the hydrothermal reactive bath at 65 - 80 ℃ for various growth time. The hydrothermal reaction solution was composed of 50 mM zinc nitrate hexahydrate ($Zn(NO_3)_2 \cdot 6H_2O$, 99.5%) and 50 mM hexamethylenetetramine (HMT, $C_6H_{12}N_4$, 99.5%), and the pH value of the mixed aqueous solution was monitored and controlled at 10.5 by the addition of ammonium hydroxide (NH_4OH) solution. After the hydrothermal synthesis process, the samples were rinsed with DI water and dried under nitrogen flow. Some of the obtained ZnO nanowire samples were annealed isothermally in vacuum (< 2 ×

10^{-2} torr) and then in a high purity O_2 ambient at 400 ℃ for 1 h.

The surface roughness of the AZO seed layers was measured using an atomic force microscope (AFM, SII Technology SPA-400). A scanning electron microscope (SEM, Hitachi S-3000H) was utilized to characterize the length and surface morphology of the ZnO nanowires grown at various reaction temperatures and for various lengths of time. The microstructural characterization and crystallographic orientation determination were carried out using an X-ray diffractometer (XRD, BRUKER, D8 Advance), a transmission electron microscope (TEM, JEOL JEM2000FXII), and the selected-area electron diffraction (SAED) technique. A high-resolution TEM (HRTEM, JEOL JEM2100) was utilized to determine the atomic structures of the synthesized ZnO nanowires. To characterize the surface wetting properties of the ZnO nanowire arrays after different heat treatments, water contact angle (CA) measurements were carried out at room temperature. A DI water droplet of 3 μL was used for each CA measurement.

3. Results and discussion

Figure 1 (a) is a representative AFM image of the sputtered AZO film after annealing in vacuum at 400 ℃, showing that the surface of the annealed AZO film was relatively smooth with the average surface roughness (R_a) being about 3.4 nm. From planview and cross-sectional TEM observations, as shown in Figs. 1 (b)-(c), it is clear that the annealed AZO film was consisted of many columnar grains with 35-50 nm size in lateral direction and elongated along the deposition direction. The arc-like SAED pattern shown in the inset of Fig. 1 (c) indicated that the AZO film

had a wurtzite structure and grew with a preferred c-axis orientation perpendicular to the substrate surface. The corresponding XRD pattern shown in Fig. 1 (d) exhibited the strong (0002) characteristic peak, which also demonstrated the preferential orientation of the AZO film along the [0001] (c-axis) direction. The highly c-axis oriented AZO film was then used as the seed layer for the hydrothermal synthesis of ZnO nanowires. Figures 2 (a)-(d) show the tilt-view SEM images of the ZnO nanowires grown on AZO seed layers under the same hydrothermal route at 65 ℃, 70 ℃, 75 ℃, and 80 ℃, respectively, for 90 min. As can be seen from the SEM images, dense and vertically-aligned ZnO nanowire arrays were successfully synthesized on all the substrates in the reaction temperature range of 65 ℃ to 80 ℃. It can also be found that the surfaces of the as-grown nanowire arrays are smooth, clean and free of precipitates or particles. The chemical reactions for the hydrothermal synthesis of ZnO nanowires can be expressed as follows[18,24] :

$$C_6H_{12}N_4 + 6H_2O \rightarrow 4NH_3 + 6CH_2O \quad (1)$$

$$NH_3 + H_2O \rightarrow NH_4^+ + OH^- \quad (2)$$

$$Zn^{2+} + 4OH^- \rightarrow Zn(OH)_4^{2-} \quad (3)$$

$$Zn(OH)_4^{2-} \rightarrow Zn(OH)_2 + 2OH^- \quad (4)$$

$$Zn(OH)_2 \rightarrow ZnO + H_2O \quad (5)$$

Based on the formation mechanism, the HMT ($C_6H_{12}N_4$) was hydrolyzed under elevated temperature to release OH^- ions. Then, the Zn^{2+} ions in the hydrothermal solution would react with the produced OH^- ions to form zinc complex ions with negative charges, which subsequently decomposed thermally to ZnO crystal. Figure 2 (e) is the XRD patterns corresponding to the ZnO

nanowire samples shown in Figs. 2 (a)-(d). In the XRD patterns, a strong and sharp diffraction peak at $2\theta = 34.5^{o}$ corresponding to (0002)ZnO was detected in all four samples, indicating that the hydrothermally synthesized ZnO nanowires also grew vertically along the [0001] direction. To further investigate the morphology and crystal structure of the synthesized ZnO nanowires, TEM, SAED, and HRTEM analyses were carried out.

Figure 3 (a) and its inset show, respectively, a representative bright-field TEM image and the corresponding SAED pattern of an as-synthesized ZnO nanowire. It is evident from the TEM image that the surface of the ZnO nanowire is relatively smooth and its diameter is quite uniform over the entire length. A closer examination further revealed that the top end of the synthesized ZnO nanowire was tapered. The detailed mechanism for the growth of tapered-tip ZnO nanowires can be found in some previous studies.[25,26] The periodic SAED spot pattern of the synthesized nanowire (as shown in the inset of Fig. 3 (a)) can be fully indexed as the $[1\bar{1}00]$ zone axis of a wurtzite ZnO crystal structure. Figure 3 (b) is the corresponding HRTEM image taken along the $[1\bar{1}00]$ zone axis from the region marked by the red square in Fig. 3 (a). The measured lattice spacing of 0.26 nm is in good agreement with the interplanar distance of the (0002) lattice plane of a pure ZnO crystal. From both SAED and HRTEM analyses, it was further confirmed that all the synthesized ZnO nanowires were single crystalline and their axial orientations were parallel to the [0001] direction, which was identical to the preferred orientation of the AZO seed layer used. It is known that the hexagonal wurtzite ZnO is a polar crystal, having two polar planes, i.e. the positively charged Zn-terminated (0001) plane and the negatively charged O-terminated $(000\bar{1})$ plane.[27] Therefore,

during the hydrothermal growth process, the produced zinc complex ions with negative charges would preferentially adsorb onto the positively charged Zn-terminated (0001) plane of AZO seed layers, promoting the subsequent growth of ZnO crystals in the [0001] (c-axis) direction and resulting in the formation of one-dimensional ZnO nanowire structure with preferred c-axial orientation. The results are consistent with those of the above SEM and XRD analyses.

For the growth kinetics study, the AZO-seeded substrates were immersed into the hydrothermal reactive bath at 65 - 80 ℃ for different periods of time and then systematically examined by cross-sectional SEM to obtain the evolution of the ZnO nanowire lengths with the hydrothermal temperatures and time. Figures 4 (a) - (g) show, respectively, the cross-sectional SEM images of ZnO nanowires grown at 80 ℃ for 60, 90, 120, 150, 180, 210, and 240 min. The corresponding plot of the average length of ZnO nanowires as a function of synthesis time at 80 ℃ is shown in Fig. 4 (h). From the SEM observations, the length of ZnO nanowires was found to increase steadily and linearly with synthesis time until 150 min and then remain roughly constant up to 240 min. The non-linear growth behavior was likely due to the high consumption of the reactant ions in solution over long periods of reaction time. Therefore, in the present study, the hydrothermal synthesis of ZnO nanowires was carried out at 65 - 80 ℃ for a time ranging from 60 to 150 min. Figures 5 (a)-(b), (c)-(d), and (e)-(f) show the cross-sectional SEM images of vertical ZnO nanowires synthesized at 65 ℃, 70 ℃, and 75 ℃ for 60 min and 150 min, respectively. It is clear from the SEM images that the synthesized ZnO nanowires are dense and vertically aligned, and their lengths increase with synthesis temperatures and time. Similar temperature- and

time-dependent growth behaviors were also observed for the other nanowire samples studied in this work.

After a series of cross-sectional SEM examinations, the evolutions of the ZnO nanowires lengths as a function of synthesis time at reaction temperatures ranging from 65 ℃ to 80 ℃ were obtained, as shown in Fig. 6 (a). It is clearly observed from Fig. 6 (a) that the lengths of the ZnO nanowires increase linearly with synthesis time at each reaction temperature, indicating that in the range of synthesis temperatures and time studied here, the hydrothermal growth of ZnO nanowires is reaction-controlled. Based on the determinations, the growth rates of ZnO nanowires were found to strongly depend on synthesis temperatures. The dependence of the growth rate (r) of ZnO nanowires on synthesis temperature (T) can be expressed by the Arrhenius equation:

$$r = A \exp(-E_a/kT)$$

where A is the pre-exponential factor, E_a is the activation energy of the ZnO nanowires growth, and k is the Boltzmann constant. Thus, by measuring the growth rates of ZnO nanowires at various reaction temperatures (i.e. the slopes of the straight fitting lines presented in Fig. 6 (a)), the activation energy for the linear growth of ZnO nanowires on AZO film-seeded substrates can be readily determined from the slope of the Arrhenius plot of logarithmic value of growth rate ($\ln r$) versus the reciprocal of the absolute reaction temperature ($1/T$). The corresponding Arrhenius plot is shown in Fig. 6 (b), and the activation energy was estimated to be about 35 kJ/mol. The obtained value was found to be smaller as compared to a previous study done by Zhou et al. (~ 80.52 kJ/mol).[18] In their study, ZnO nanorods were synthesized by homogeneous nucleation in bulk

aqueous solution at 55 - 85 ℃ for different reaction times. In contrast, in this study, the ZnO nanowires were found to preferentially nucleate and grow on AZO film-seeded substrates without precipitation in the bulk solution. It has been demonstrated in several previous studies that the heterogeneous nucleation of crystalline phases on substrates is much easier than the homogeneous nucleation in solutions, since the interfacial energy between crystals and substrates is usually smaller than that between crystals and solutions.[28-30] A reduction in the interfacial energy can be sufficient to strongly favor heterogeneous over homogeneous nucleation. Thus, for the growth of ZnO nanowires in the hydrothermal solution, the heterogeneous nucleation takes place preferentially on the surface of AZO seed layer due to the reduced nucleation barrier by decreasing the interfacial energy. Therefore, the discrepancy in the activation energy value between Zhou et al.'s study and ours can be explained by the different nucleation mechanisms.

The surface wettability of ZnO nanowire samples after different treatments was evaluated by measurement of the water contact angle. As can be seen in Fig. 7 (a), the as-synthesized ZnO nanowires were hydrophilic in nature with a contact angle of about 10^{o}. The hydrophilic nature is likely due to the presence of OH^- groups and oxygen related defects (e.g. O^-) on the surfaces of ZnO nanowires created during the hydrothermal synthesis process.[31,32] These defects could interact with H_2O molecules, enhancing the hydrophilicity of nanowire surfaces. However, these defects are not stable. Thus, it could be expected that when the as-synthesized ZnO nanowire samples were stored in an atmospheric ambient environment sufficiently long enough, the nanowire surfaces would transform into a more energetically stable state. It is evident from the contact angle measurements

shown in Fig. 7 (a) that after being stored in a common box (closed but not sealed) under regular atmospheric ambient (normal environment) for various lengths of time, the surface of ZnO nanowires gradually changed from hydrophilic to hydrophobic. The water contact angle values were found to gradually increase from initial 10^{o} to about 110^{o} with increasing the storage time up to 30 days. The variation of water contact angles of ZnO nanowire samples as a function of the storage time is shown in Fig. 7 (b).

In addition, the surface wettability of ZnO nanowires was also found to be significantly affected by the heat treatment conditions. Figure 8 (a) shows the representative optical images of water droplets on the surfaces of as-synthesized ZnO nanowire samples after alternating annealing in vacuum and in a high purity O_2 ambient at 400 ℃ for 1 h. It can be clearly seen that after annealing in vacuum, the as-synthesized ZnO nanowires surface became highly hydrophobic with the water contact angle increasing from initial 10^{o} to about 105^{o}. The dramatic conversion of ZnO nanowires surface from hydrophilic to hydrophobic could be attributed to the enhanced desorption of surface OH^- groups and H_2O molecules during the vacuum annealing.[33] When the vacuum-annealed samples were further annealed in oxygen atmosphere, as shown in Fig. 8 (a), the surface wettability of ZnO nanowires returned back to its pristine hydrophilic state with lower water contact angles. Several previous studies have suggested that the hydrophilic properties of ZnO materials could be attributed to the formation of high density of oxygen vacancies on the ZnO surfaces.[22,23] Recently, however, Zhang et al.[32] reported a detailed XPS study on the ZnO nanorod surfaces after annealing in air at different temperature for 1 h. According to their XPS study of O 1s

spectra, the O-vacancy concentration in the ZnO nanorods was gradually decreased with increasing air-annealing temperature up to 650 ^{o}C, while the concentration of the absorbed H_2O on the ZnO nanorod surfaces was found to maintain the same high level. The XPS results suggest that the water contact angle of the air-annealed ZnO nanorod surfaces can retain at lower value even after annealing at 650 ^{o}C, and further indicate that the hydrophilicity of ZnO nanorods is not related to the oxygen vacancy. Indeed, in this study, we have demonstrated that after annealing in O_2 atmosphere at 400 ^{o}C for 1 h, the ZnO nanowires surface became highly hydrophilic with lower water contact angles. It is known that the water contact angle typically will decrease as the surface energy of solid materials increases. Thus, it can be expected that during O_2 annealing, the O_2 molecule could dissociate at an O-vacancy site and fill the O-vacancy with one dissociated O atom. The other O atom would thereby become an O adatom on the ZnO nanowire surface. These oxygen adatoms and oxygen related defects created by O_2 annealing make the ZnO nanowire surfaces have high surface energy, which results in hydrophilic surfaces with lower water contact angles. Furthermore, the wettability conversion of ZnO nanowires can be reversibly manipulated by alternate annealing in vacuum and oxygen atmospheres. The corresponding variation of water contact angles of ZnO nanowire samples under repeated alternation of vacuum and oxygen annealing is shown in Fig. 8 (b). Since controlling the wettability of solid surfaces is a key issue in surface engineering, the above heat treatment approach to manipulate the ZnO nanowires with switchable surface wettability presented in this study provides the capability to extend the practical applications of ZnO materials to various interesting subjects.

4. Conclusions

In summary, vertically-aligned, length-tunable ZnO nanowire arrays with controllable surface wettability have been successfully synthesized on AZO-seeded substrates by controlling the hydrothermal temperatures and time, and the post-heat treatments. The results of XRD, TEM, SAED, and HRTEM analyses indicated that all the as-synthesized ZnO nanowires were single crystalline with a wurtzite structure and their growth directions were along the [0001] (the c-axis), which was identical to the preferred orientation of the AZO seed layer used. From cross-sectional SEM observations, the length of the ZnO nanowires was found to be linearly proportional to the synthesis time in the temperature range studied, indicating that the hydrothermal growth of ZnO nanowires was reaction-controlled. The activation energy for the linear growth of vertical ZnO nanowires on AZO-seeded substrates could be derived from the Arrhenius plot and it was found to be about 35 kJ/mol, which was smaller than that of ZnO nanowires synthesized in bulk solution. Water contact angle measurements revealed that the as-synthesized ZnO nanowires exhibited a hydrophilic characteristic, and their surface wettability was significantly affected by the storage time and heat treatment conditions. Furthermore, the wettability of ZnO nanowires could be adjusted by alternate annealing in vacuum and oxygen atmospheres, and the wettability conversion was fully reversible and controllable.

Acknowledgment

The research was supported by the Ministry of Science and Technology of Taiwan, R.O.C..

Notes and references

1. J. G. Lu, P. C. Chang, and Z. Y. Fan, *Mater. Sci. Eng. R-Rep.*, 2006, **52**, 49.
2. B. Liang, H. T. Huang, Z. Liu, G. Chen, G. Yu, T. Luo, L. Liao, D. Chen, and G. Z. Shen, *Nano Res.*, 2014, **7**, 272.
3. S. H. Ko, D. Lee, H. W. Kang, K. H. Nam, J. Y. Yeo, S. J. Hong, C. P. Grigoropoulos, and H. J. Sung, *Nano Lett.*, 2011, **11**, 666.
4. Y. Xi, J. H. Song, S. Xu, R. S. Yang, Z. Y. Gao, C. G. Hu, and Z. L. Wang, *J. Mater. Chem.*, 2009, **19**, 9260.
5. C. S. Chou, Y. C. Wu, and C. H. Lin, *RSC Adv.*, 2014, **4,** 52903.
6. S. Suhaimi, S. Sakrani, T. Dorji, and A. K. Ismail, *Nanoscale Res. Lett.*, 2014, **9**, 256.
7. M. A. Susner, S. D. Carnevale, T. F. Kent, L. M. Gerber, P. J. Phillips, M. D. Sumption, and R. C. Myers, *Physica E*, 2014, **62**, 95.
8. S. Ashraf1, A. C. Jones, J. Bacsa, A. Steiner, P. R. Chalker, P. Beahan, S. Hindley, R. Odedra, P. A. Williams, and P. N. Heys, *Chem. Vapor Depos.*, 2011, **17**, 45.
9. H. M. Cheng, W. H. Chiu, C. H. Lee, S. Y. Tsai, and W. F. Hsieh, *J. Phys. Chem. C*, 2008, **112**, 16359.
10. M. J. Zheng, L. D. Zhang, G. H. Li, and W. Z. Shen, *Chem. Phys. Lett.*, 2002, **363**, 123.
11. J. Elias, R. Tena-Zaera, and C. Levy-Clement, *Thin Solid Films*, 2007, **515**, 8553.
12. J. M. Wang and L. Gao, *Solid State Commun.*, 2004, **132**, 269.
13. H. F. Li, X. H. Zhang, Y. Q. Zhu, R. Li, H. Y. Chen, P. Gao, Y. Y. Zhang, T. T. Li, Y. N. Liu, and Q. W. Li, *RSC Adv.*, 2014, **4,** 43772.
14. S. N. Bai, H. H. Tsai, and T. Y. Tseng, *Thin Solid Films*, 2007, **516**, 155.

15. J. Song and S. Lim, *J. Phys. Chem. C*, 2007, **111**, 596.

16. J. Hu, Y. J. Sun, W. D. Zhang, F. Q. Gao, P. W. Li, D. Jiang, and Y. Chen, *Appl. Surf. Sci.*, 2014, **317**, 545.

17. Z. K. Li, X. T. Huang, J. P. Liu, Y. Y. Li, and G. Y. Li, *Mater. Lett.*, 2008, **62**, 1503.

18. Z. Z. Zhou and Y. L. Deng, *J. Phys. Chem. C*, 2009, **113**, 19853.

19. Z. Q. Sun, T. Liao, K. S. Liu, L. Jiang, J. H. Kim, and S. X. Dou, *Small*, 2014, **10**, 3001.

20. L. B. Feng, L. B. Zhao, X. H. Qiang, Y. H. Liu, Z. Q. Sun, and B. Wang, *Appl. Phys. A*, 2015, **119,** 75.

21. F. R. Wang, G. Q. Zhang, Z. Zhao, H. Q. Tan, W. X. Yu, X. M. Zhang, and Z. C. Sun, *RSC Adv.*, 2015, **5,** 9861.

22. D. Sirbu, A. P. Rambu, and G. I. Rusu, *Mater. Sci. Eng. B*, 2011, **176,** 266.

23. H. Hu, H. F. Jib, and Y. Sun, *Phys.Chem. Chem. Phys.*, 2013, **15,** 16557.

24. G. M. Hua, Y. Tian, L. L. Yin, and L. D. Zhang, *Cryst. Growth Des.*, 2009, **9**, 4653.

25. R. A. Laudise and A. A. Ballman, *J. Phys. Chem.*, 1960, **64,** 688.

26. Z. Q. Zhang and J. Mu, *J. Colloid Interf. Sci.*, 2007, **307,** 79.

27. G. Perillat-Merceroz, R. Thierry, P. H. Jouneau, P. Ferret, and G. Feuillet, *Nanotechnology*, 2012, **23,** 125702

28. B. C. Bunker, P. C. Rieke, B. J. Tarasevich, A. A. Campbell,G. E. Fryxell, G. L. Graff, L. Song, J. Liu, J. W. Virden, and G. L. McVay, *Science*, 1994, **264,** 48.

29. Y. X. Li, M. Guo, M. Zhang, and X. D. Wang, *Mater. Res. Bull.*, 2009, **44,** 1232.

30. L. Vayssieres, K. Keis, S. E. Lindquist, and A. Hagfeldt, *J. Phys. Chem. B*, 2001, **105,** 3350.

31. A. B. Gurav, S. S.Latthe, R. S.Vhatkar, J. G. Lee, D. Y. Kim, J. J. Park, and S. S. Yoon, *Ceram. Int.*, 2014, **40**, 7151.

32. J. Zhang, Y. R. Liu, Z. Y. Wei, and J. Y. Zhang, *Appl. Surf. Sci.*, 2013, **265**, 363.

33. J. J. Qiu, X. M. Li, W. Z. He, S. J. Park, H. K. Kim, Y. H. Hwang, J. H. Lee, and Y. D. Kim, *Nanotechnology*, 2009, **20**, 155603.

Figure captions

Fig. 1. (a) AFM image, (b) planview TEM image, (c) cross-sectional TEM image, and (d) XRD spectrum of the sputtered AZO seed layer after annealing in vacuum at 400 ℃ for 1 h. The inset of (c) is the corresponding SAED pattern.

Fig. 2. (a) - (d) Tilt-view SEM images and (e) the corresponding XRD patterns of the ZnO nanowires grown on AZO seed layers at various synthesized temperatures for 90 min (scale bar = 2 μm). (a) 65 ℃, (b) 70 ℃, (c) 75 ℃, and (d) 80 ℃.

Fig. 3. (a) A representative bright-field TEM image and the corresponding indexed SAED pattern of an as-synthesized ZnO nanowire. (b) HRTEM image taken from the region outlined by the red square in (a).

Fig. 4. Cross-sectional SEM images of vertical ZnO nanowires grown on AZO seed layers at 80 ℃ for (a) 60 min, (b) 90 min, (c) 120 min, (d) 150 min, (e) 180 min, (f) 210 min, and (g) 240 min (scale bar = 3 μm). (h) A plot of the average length of ZnO nanowires as a function of synthesis time at 80 ℃.

Fig. 5. Cross-sectional SEM images of vertical ZnO nanowires grown on AZO seed layers at (a) - (b) 65 ℃, (c) - (d) 70 ℃, and (e) - (f) 75 ℃ (scale bar = 3 μm). The corresponding synthesis times were: (a), (c), (e) 60 min; (b), (d), (f) 150 min.

Fig. 6. (a) The average length of ZnO nanowires versus synthesis time curves for the samples hydrothermally synthesized at 65 - 80 ℃. (b) Arrhenius plot of $\ln r$ versus the reciprocal of absolute synthesis temperature ($1/T$).

Fig. 7. (a) Representative photographs of water droplets on the surfaces of the ZnO nanowire samples stored in an atmospheric ambient environment at room temperature for various time intervals. (b) Variation of water contact angles of the ZnO nanowire samples with storage time.

Fig. 8. (a) Representative photographs of water droplets on the surfaces of as-synthesized ZnO nanowire samples after alternating annealing in vacuum and O_2 at 400 ℃ for 1 h. (b) The corresponding water contact angles of the ZnO nanowire samples after different heat treatments.

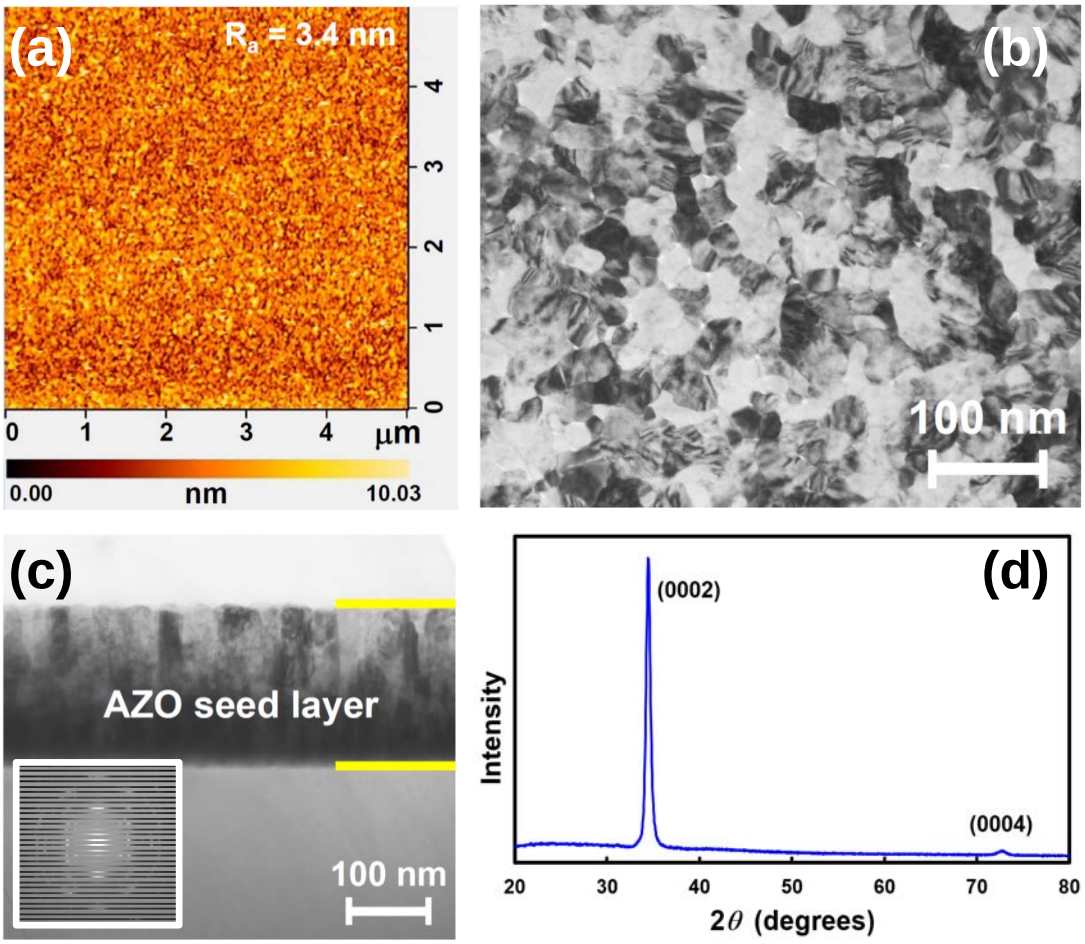

Fig. 1

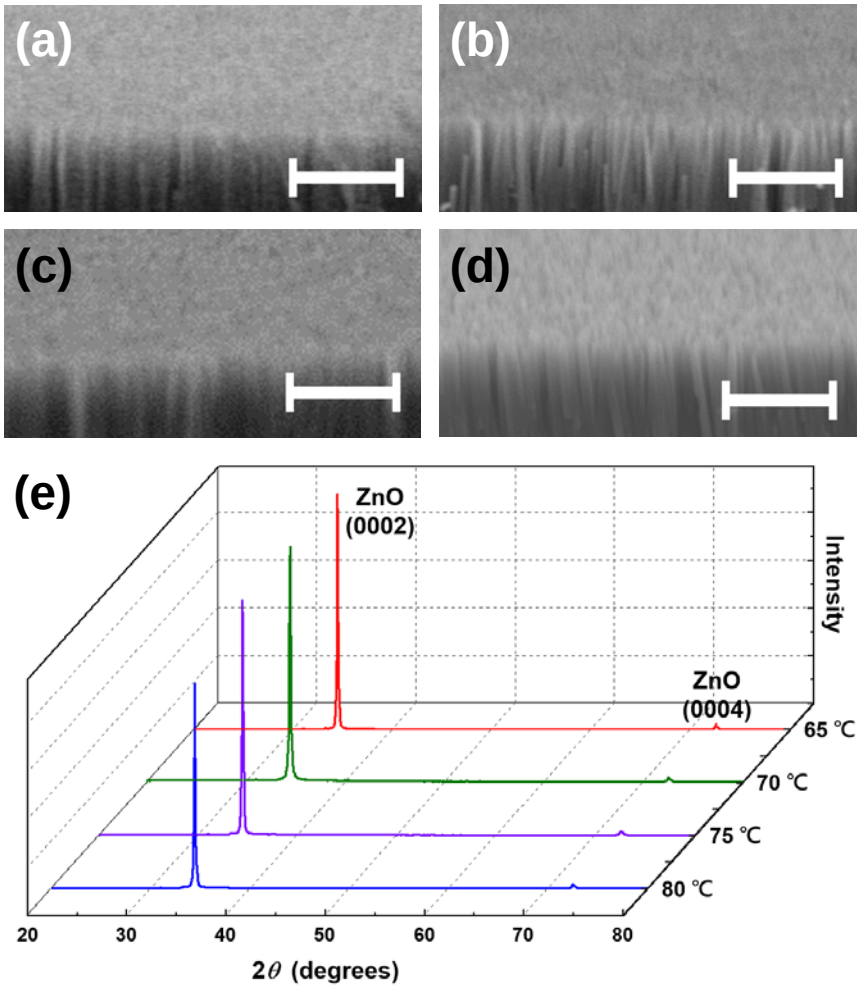

Fig. 2

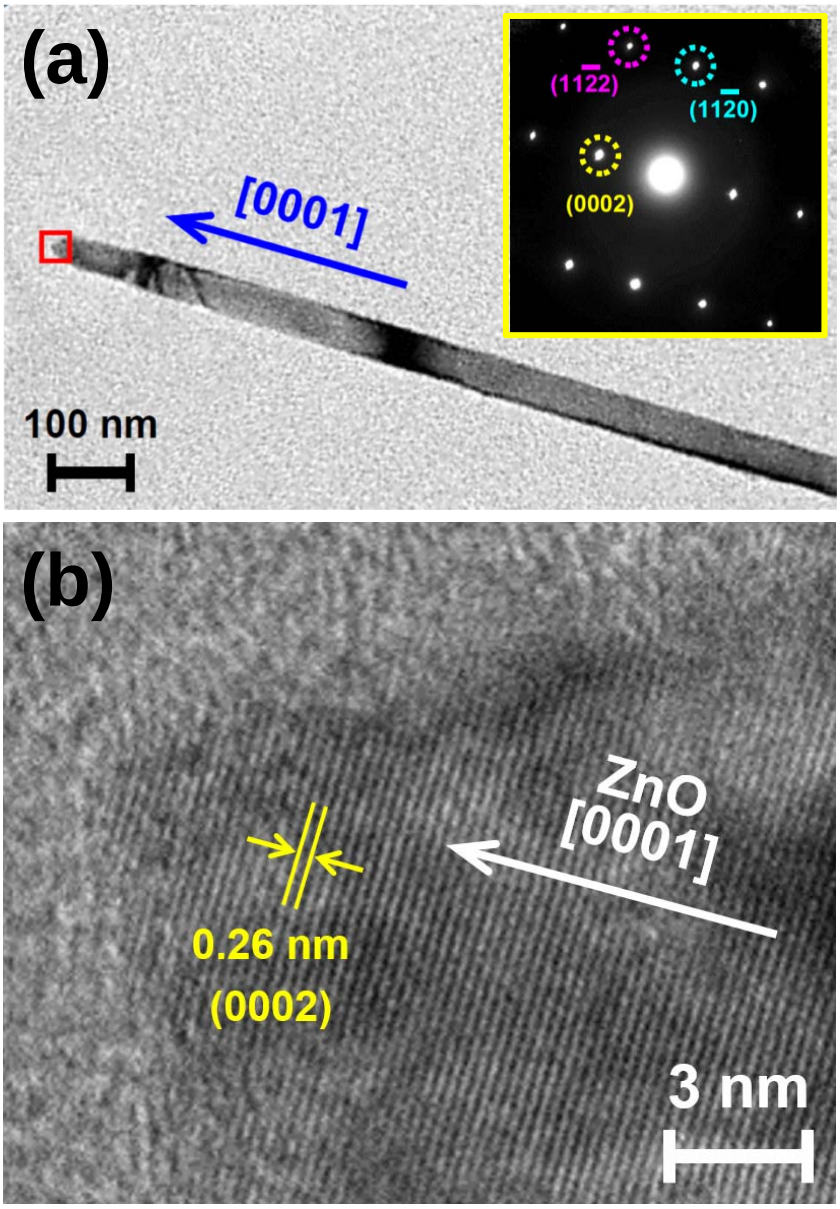

Fig. 3

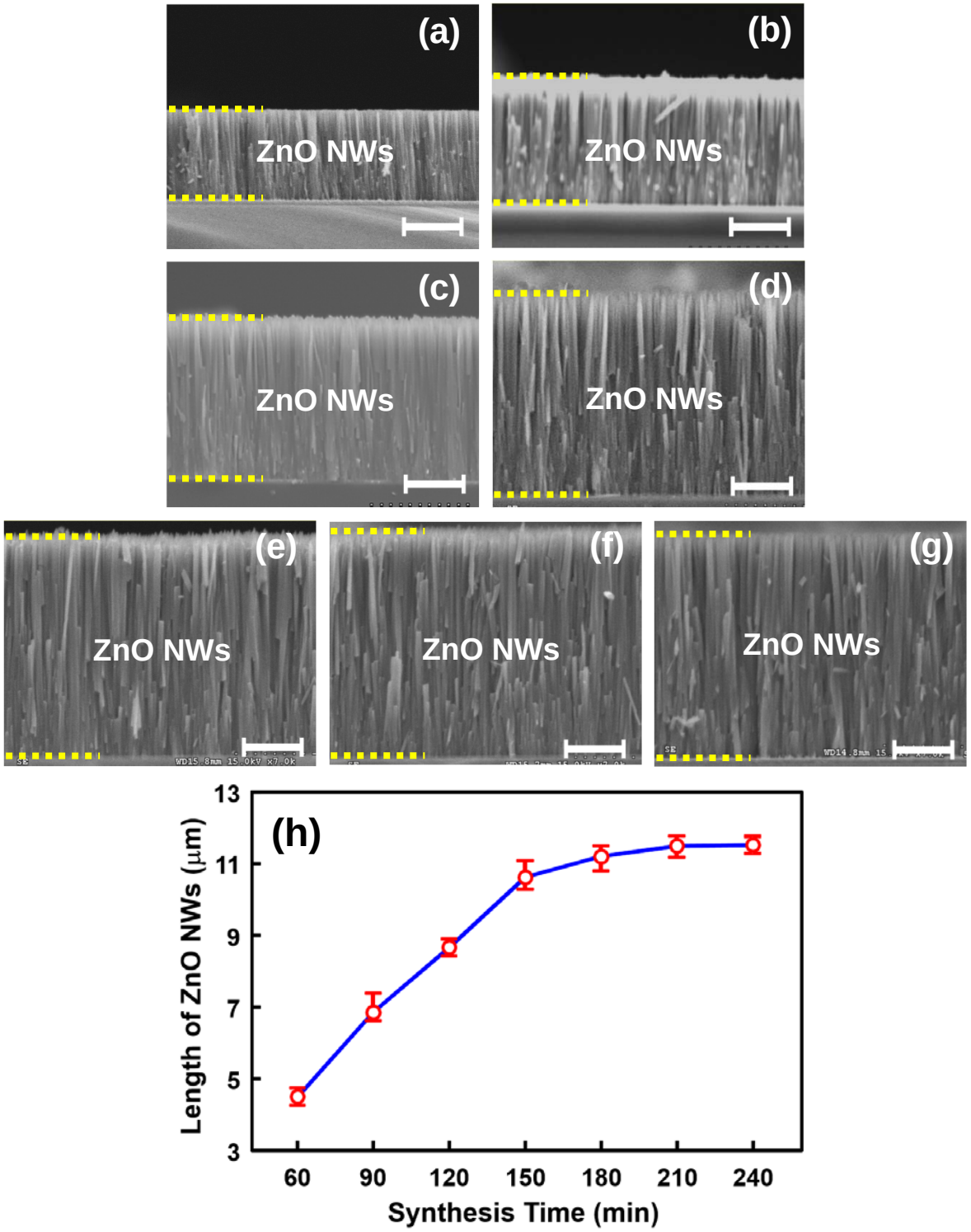

Fig. 4

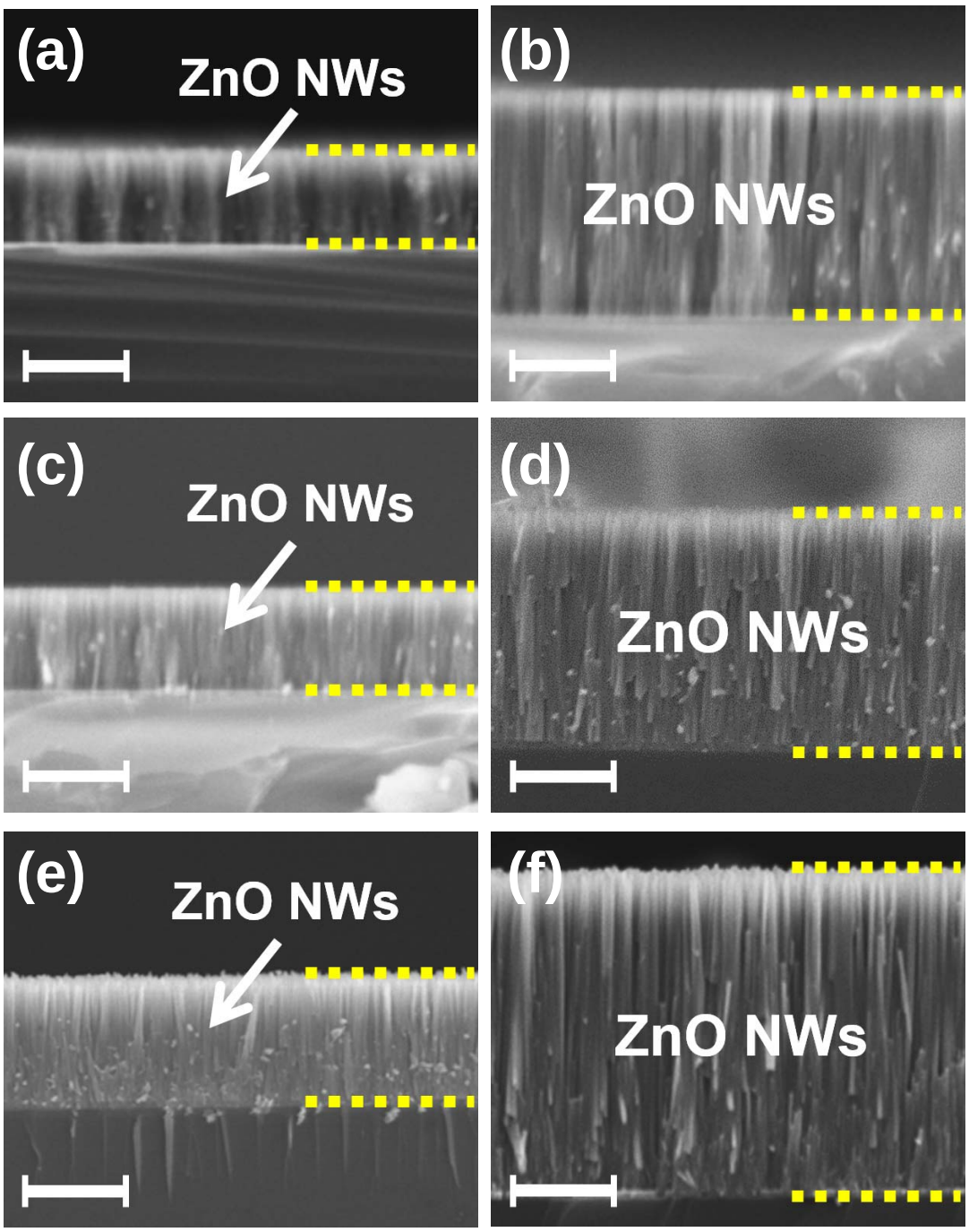

Fig. 5

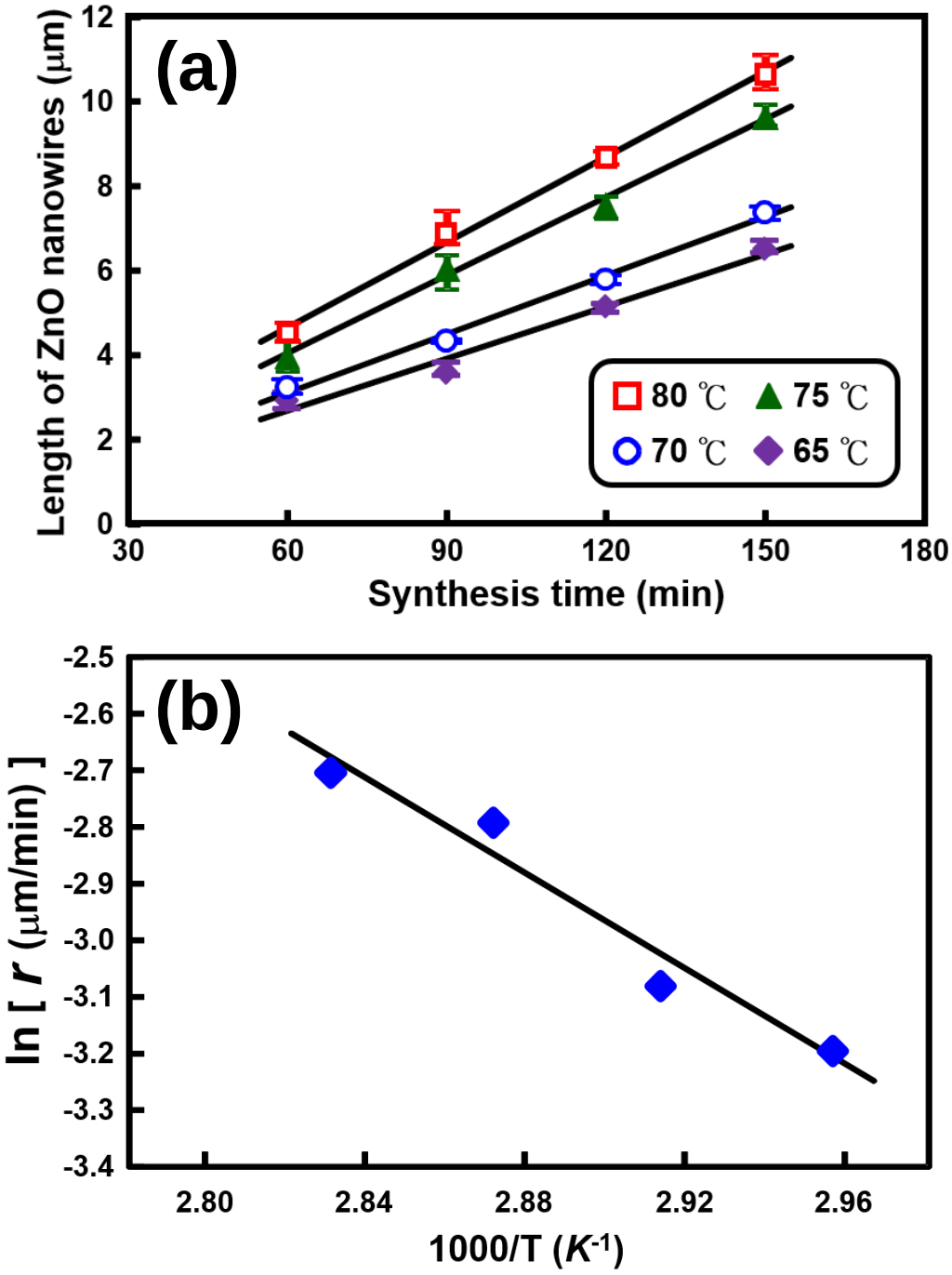

Fig. 6

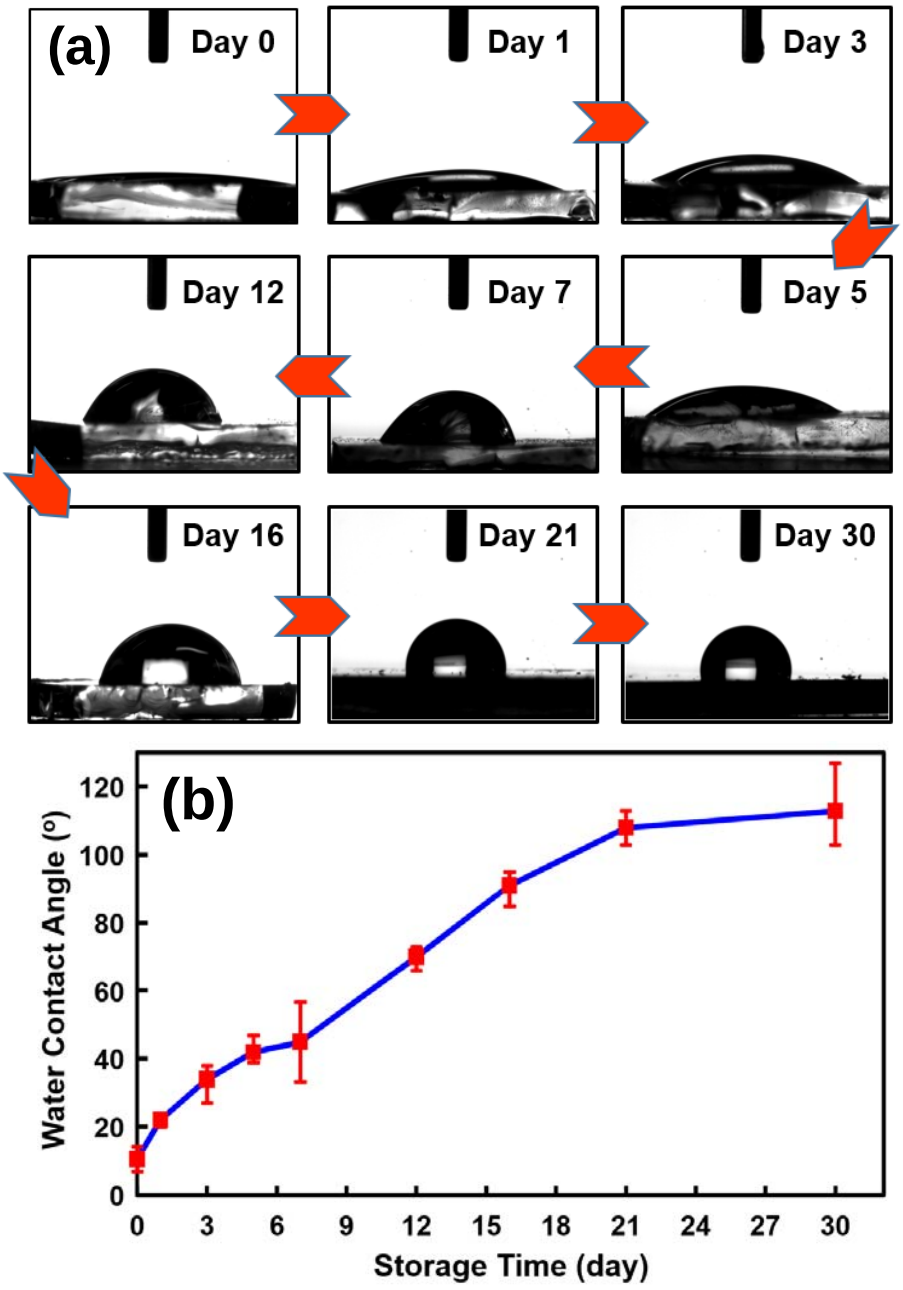

Fig. 7

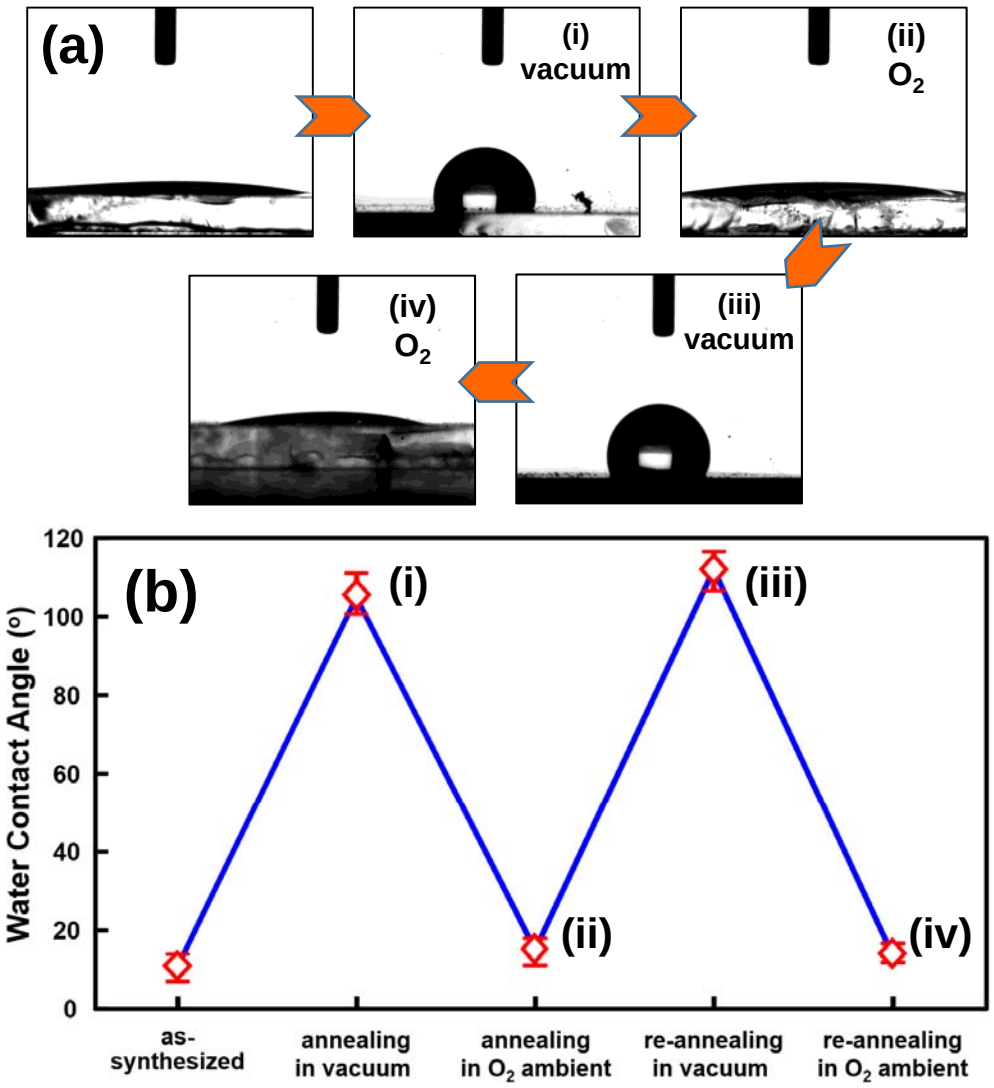

Fig. 8